Hindawi Publishing Corporation
EURASIP Journal on Wireless Communications and Networking
Volume 2008, Article ID 541410, 13 pages
doi:10.1155/2008/541410

Research Article

Zero-Forcing and Minimum Mean-Square Error Multiuser Detection in Generalized Multicarrier DS-CDMA Systems for Cognitive Radio

Lie-Liang Yang[1] and Li-Chun Wang[2]

[1] *School of Electronics and Computer Science, University of Southampton SO17 1BJ, UK*
[2] *Department of Communications Engineering, National Chiao Tung University, Hsinchu 300, Taiwan*

Correspondence should be addressed to Lie-Liang Yang, lly@ecs.soton.ac.uk

Received 30 April 2007; Revised 15 September 2007; Accepted 17 November 2007

Recommended by Luc Vandendorpe

In wireless communications, multicarrier direct-sequence code-division multiple access (MC DS-CDMA) constitutes one of the highly flexible multiple access schemes. MC DS-CDMA employs a high number of degrees-of-freedom, which are beneficial to design and reconfiguration for communications in dynamic communications environments, such as in the cognitive radios. In this contribution, we consider the multiuser detection (MUD) in MC DS-CDMA, which motivates lowcomplexity, high flexibility, and robustness so that the MUD schemes are suitable for deployment in dynamic communications environments. Specifically, a range of low-complexity MUDs are derived based on the zero-forcing (ZF), minimum mean-square error (MMSE), and interference cancellation (IC) principles. The bit-error rate (BER) performance of the MC DS-CDMA aided by the proposed MUDs is investigated by simulation approaches. Our study shows that, in addition to the advantages provided by a general ZF, MMSE, or IC-assisted MUD, the proposed MUD schemes can be implemented using modular structures, where most modules are independent of each other. Due to the independent modular structure, in the proposed MUDs one module may be reconfigured without yielding impact on the others. Therefore, the MC DS-CDMA, in conjunction with the proposed MUDs, constitutes one of the promising multiple access schemes for communications in the dynamic communications environments such as in the cognitive radios.

Copyright © 2008 L.-L. Yang and L.-C. Wang. This is an open access article distributed under the Creative Commons Attribution License, which permits unrestricted use, distribution, and reproduction in any medium, provided the original work is properly cited.

1. INTRODUCTION

Recently, there has been an increasing interest in cognitive and software defined radios in both the research and industry communities, as is evidenced, for example, by [1–4] as well as by the references in them. The cognitive radio equipped with flexible software defined architectures aims at the intelligent wireless communications, which is capable of sensing its environment, learning from the environment, and adaptively responding to the environment, in order to achieve high-efficiency and high-flexibility wireless communications anytime, anywhere, and in anyway. In cognitive and software defined radios, a highly efficient and flexible multiple access scheme that is suitable for online reconfigurations is highly important.

In broadband wireless communications, multicarrier code-division multiple access (CDMA) scheme has received wide attention in recent years [5–12]. This is because multicarrier CDMA schemes employ a range of advantages, which include low intersymbol interference (ISI) due to invoking serial-to-parallel (S-P) conversion at the transmitter, low implementation complexity of carrier modulation/demodulation for the sake of using fast Fourier transform (FFT) techniques, and so forth. In multicarrier CDMA systems, frequency diversity may be achieved by repeating the transmitted signal in the frequency *(F)* domain with the aid of several subcarriers [5, 7–9]; multiple transmit/receive antennas may be deployed, in order to achieve the spatial diversity [6, 13] and/or to increase the capacity of the multicarrier CDMA systems [14]. In comparison with the pure DS-CDMA using only time *(T)* domain spreading and pure MC-CDMA using only *F* domain spreading, it has been demonstrated that the multicarrier direct sequence CDMA (MC DS-CDMA) has the highest flexibility [5, 15] and the

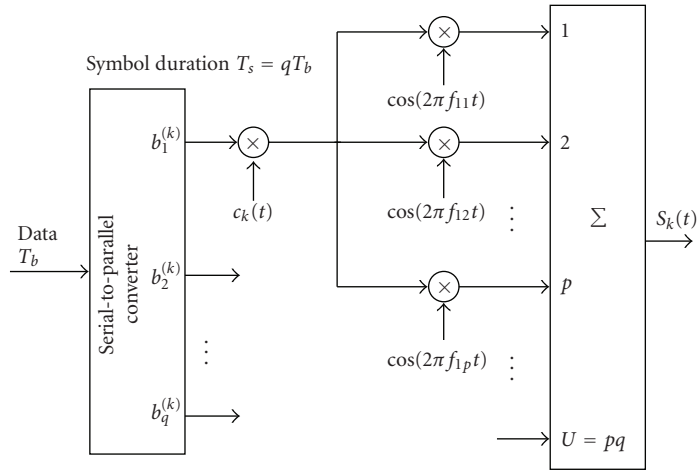

Figure 1: Transmitter schematic block diagram of the kth user in the generalized MC DS-CDMA systems.

highest number of degrees-of-freedom [5] for reconfigurations; these properties may render the MC DS-CDMA a versatile multiple access scheme that is suitable for cognitive and software-defined radios. Note that the orthogonal frequency-division multiplexing, code-division multiplexing (OFDM-CDM) scheme [16], which employs both T domain and F domain spreadings, may also constitute a high-flexible scheme that is suitable for reconfigurations.

Multiuser detection (MUD) in the context of various multicarrier CDMA schemes has been widely investigated, as seen, for example, in [17–21]. This contribution motivates low-complexity, high-reliability, and low-sensitivity MUD in the MC DS-CDMA operated under the cognitive radio. This is because in a highly dynamic wireless communications environment, such as in cognitive radio, low-complexity, high-reliability, and robustness to imperfect knowledge due to, for example, channel estimation error are extremely important. Specifically, in this contribution we investigate the zero-forcing MUD (ZF-MUD) and minimum mean-square error MUD (MMSE-MUD) in the MC DS-CDMA systems. Various alternatives for implementation of the ZF-MUD and MMSE-MUD are proposed. To be more specific, in this contribution three types of ZF-MUDs and four types of MMSE-MUDs are proposed. The ZF-MUDs include the optimum ZF-MUD (OZF-MUD), suboptimum ZF-MUD (SZF-MUD), as well as the interference cancellation aided suboptimum ZF-MUD (SZF-IC). The MMSE-MUDs include the optimum MMSE-MUD (OMMSE-MUD), suboptimum MMSE-MUD type I and II (SMMSE-MUD-I, SMMSE-MUD-II) and the interference cancellation aided suboptimum SMMSE-MUD-II (SMMSE-IC). From our study it can be shown that in MC DS-CDMA systems both the ZF-MUDs and MMSE-MUDs have the modular structures that are beneficial to implementation and reconfiguration. Furthermore, in this contribution the bit-error rate (BER) performance of the MC DS-CDMA systems employing the proposed various MUDs is investigated by simulations. From our study and simulation results, it can be shown that among these MUDs, the SZF-MUD, SZF-IC, and the SMMSE-MUD-II, SMMSE-IC, constitute the promising MUD schemes that can provide the following advantages.

(i) Low complexity. The complexity of these MUDs is in the order of the single-user matched-filter- (MF-) based detector, when the active users in the MC DS-CDMA system are maintained unchanged.

(ii) High efficiency. Both SZF-MUD and SMMSE-MUD-II are capable of mitigating efficiently the multiuser interference (MUI), although their achievable BER performance is worse than that of their corresponding OZF-MUD and OMMSE-MUD. However, when an IC-stage is invoked following the SZF-MUD or SMMSE-MUD-II, the SZF-IC or SMMSE-IC is capable of achieving the near single-user BER bound achieved by the MC DS-CDMA supporting single-user.

(iii) Robust to imperfect channel knowledge. In the above four types of MUDs, the time-variant channel impulse responses (CIRs) are only invoked in linear operations as in MF-assisted detection. No channel-dependent matrices need to be inverted. Hence, we can be implied that these MUDs should have a similar sensitivity as the MF detector to the channel estimation errors.

(iv) High-flexibility. Due to the modular structures and the relative independence among the modules, these MUDs are highly flexible. For example, if some of the subcarriers are sensed with high interference temperature, these MUD algorithms can be readily modified to adapt the environment, as can be seen in our forthcoming discourses.

The remainder of this contribution is organized as follows. Section 2 describes the MC DS-CDMA system in the context of its transmitter and receiver models. In this section, the desirable representations for the observations at the receiver are also provided. Section 3 derives the ZF-MUDs, while Section 4 considers the MMSE-MUDs. In Section 6 the simulation results are provided, while, finally, in Section 7 we present our conclusions.

2. SYSTEM DESCRIPTION

In this section, the considered MC DS-CDMA system is described in the context of the transmitted signal, channel model, receiver, as well as the representation of the received discrete signals. Let us first describe the transmitter of the MC DS-CDMA system.

2.1. Transmitted signals

The transmitter schematic diagram of the kth user in the considered MC DS-CDMA is shown in Figure 1. As shown in Figure 1 the initial data stream having a bit duration of T_b is first serial-to-parallel (S-P) converted to q number of lower-rate substreams. Hence, the new bit duration after the S-P conversion or the symbol duration is $T_s = qT_b$. Each of the q lower-rate substreams is spread by $c_k(t)$ of the kth user's signature sequence. As shown in Figure 1, each of the q substreams is transmitted by p number of subcarriers, in order for achieving a pth order frequency diversity. Hence, the total number of subcarriers required by the MC DS-CDMA system is $U = pq$. Based on Figure 1, the transmitted signal of user k can be expressed as

$$s_k(t) = \sum_{i=1}^{q}\sum_{j=1}^{p}\sqrt{\frac{2P}{p}}b_i^{(k)}(t)c_k(t)\cos\left(2\pi f_{ij}t + \phi_{ij}^{(k)}\right), \quad k = 1,2,\ldots,K, \tag{1}$$

where P is the transmitted power of each substream, $b_i^{(k)}(t) = \sum_{n=-\infty}^{\infty} b_i^{(k)}[n]P_{T_s}(t - nT_s)$ $(i = 1,\ldots,q)$ represents the binary data of the ith substream, where $b_i^{(k)}[n]$ is assumed to be a random variable taking values of $+1$ or -1 with equal probability, while $P_\tau(t)$ represents the rectangular waveform. In (1) $c_k(t)$ represents the spreading code assigned to the kth user, which is the same for all the $U = pq$ number of subcarriers. The spreading sequence $c_k(t)$ can be expressed as $c_k(t) = \sum_{j=-\infty}^{\infty} c_j^{(k)}\psi(t - jT_c)$, where $c_j^{(k)}$ assumes values of $+1$ or -1, while $\psi(t)$ is the T domain chip waveform of the spreading sequence, which is defined over the interval $[0, T_c)$ and normalized to $\int_0^{T_c}\psi^2(t)dt = T_c$. Furthermore, $N_e = T_s/T_c = qT_b/T_c$ is defined as the spreading factor on each of the subcarriers. Finally, in (1) $\phi_{ij}^{(k)}$ represents the initial phase associated with the carrier modulation with respect to the subcarrier determined by (i, j) in (1).

In the considered MC DS-CDMA, we assume that the subcarrier signals are configured so that the subcarrier signals are orthogonal with each other at the chip-level. This condition can be achieved, for example, by letting the spacing between two adjacent subcarriers be $\Delta = 1/T_c$ or $\Delta = 2/T_c$ [7, 8, 11]. We assume that the bandwidth of each subcarrier signal is configured to be sufficiently narrow in comparison with the coherence bandwidth of the wireless channel, so that each subcarrier signal experiences flat fading. As shown in [5], this configuration can be implemented by changing the total number of subcarriers qp, the spacing between two adjacent subcarriers and/or the number of bits q invoked in the S-P conversion. Furthermore, we assume that the subcarriers are arranged in such a way that the subcarriers conveying the same data bit, as shown in Figure 1, are separated as far away as possible, in order to achieve possibly the highest F domain diversity. Note that, in our simulations we assume for simplicity that the subcarriers conveying the same data bit experience independent fading.

Let us assume that the MC DS-CDMA system supports K number of users, which communicate with one common base-station (BS) synchronously. The average power received from each user at the BS is also assumed to be the same. Furthermore, we assume that the MC DS-CDMA signals experience frequency-selective Rayleigh fading, but each of the subcarrier signals experiences flat Rayleigh fading. Consequently, when K signals obeying the form of (1) are transmitted over the above-mentioned channels, the received baseband equivalent signal at the BS can be expressed as

$$R(t) = \sum_{k=1}^{K}\sum_{i=1}^{q}\sum_{l=1}^{p}\sqrt{\frac{2P}{p}}h_{il}^{(k)}b_i^{(k)}(t)c_k(t)\exp\left(j2\pi f_{il}t\right) + n(t), \tag{2}$$

where $h_{il}^{(k)}$ represents the channel gain with respect to the ilth subcarrier of the kth user, while $n(t)$ is the complex baseband equivalent Gaussian noise, which has mean-zero and a single-sided power spectral-density of N_0 per real dimension. Note that, without loss of any generality, in (2) the initial phases of the subcarriers have been absorbed into the channel gains.

2.2. Representation of the received signal

The receiver structure for detection of the MC DS-CDMA signal is shown in Figure 2. The receiver first executes the multicarrier demodulation, which can usually be implemented by the FFT techniques [22]. Following the multicarrier demodulation, a chip waveform matched-filter (MF) with the T domain impulse response $\psi^*(T_c - t)$ is employed by each of the subcarrier branches. Finally, as shown in Figure 2, the chip waveform MFs outputs are sampled at the chip-rate in order to provide the discrete observations for detection.

According to Figure 2, it can be shown that the nth observation with respect to the first transmitted MC DS-CDMA symbol and the uvth subcarrier can be expressed as

$$y_{uv,n} = \left(\sqrt{2PN_e}T_c\right)^{-1}\int_{nT_c}^{(n+1)T_c} R(t)\exp\left(-j2\pi f_{uv}t\right)\psi^*(t)dt, \quad n = 0,1,\ldots,N_e-1,\ v = 1,2,\ldots,p,\ u = 1,2,\ldots,q. \tag{3}$$

Upon substituting (2) into (3) and using the assumption that the subcarrier signals are orthogonal at the chip-level, it can be shown that $y_{uv,n}$ can be expressed as

$$y_{uv,n} = \sum_{k=1}^{K}\frac{1}{\sqrt{N_e p}}h_{uv}^{(k)}c_n^{(k)}b_u^{(k)}[0] + N_{uv,n}, \quad n = 0,1,\ldots,N_e-1, \quad v = 1,2,\ldots,p,\ u = 1,2,\ldots,q, \tag{4}$$

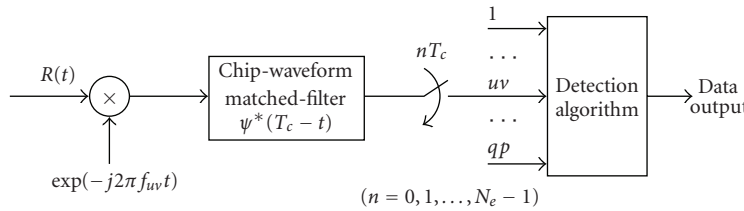

Figure 2: The receiver block diagram of the MC DS-CDMA systems using time-limited chip waveforms.

where $N_{uv,n}$ represents the Gaussian noise given by

$$N_{uv,n} = \left(\sqrt{2PN_e}T_c\right)^{-1} \int_{nT_c}^{(n+1)T_c} n(t)\exp\left(-j2\pi f_{uv}t\right)\psi^*(t)dt \tag{5}$$

which is Gaussian distributed with mean-zero and a variance of $\sigma^2/2 = N_0/2E_b$ per real dimension.

From (4) we notice that there is no inter-carrier interference (ICI), yielding that there is no interference among the bits transmitted on different subcarriers. Hence, it is sufficient for us to consider the detection of the K bits—each of which is transmitted by one of the K users—transmitted on the same p number of subcarriers. Specifically, in our forthcoming discourse we consider the detection of the uth bits of the K users, which are transmitted by the subcarriers indexed by $f_{u1}, f_{u2}, \ldots, f_{up}$.

Let us now represent the observations in (4) in some desired forms, so that they can be conveniently applied in our forthcoming derivations. Let us define

$$\begin{aligned}
\mathbf{y}_{uv} &= \left[y_{uv,0}, y_{uv,1}, \ldots, y_{uv,N_e-1}\right]^T,\\
\mathbf{n}_{uv} &= \left[N_{uv,0}, N_{uv,1}, \ldots, N_{uv,N_e-1}\right]^T,\\
\mathbf{c}_k &= \frac{1}{\sqrt{N_e}}\left[c_0^{(k)}, c_1^{(k)}, \ldots, c_{N_e-1}^{(k)}\right]^T.
\end{aligned} \tag{6}$$

Then, $\mathbf{y}_{uv}$ can be represented

$$\mathbf{y}_{uv} = \sum_{k=1}^{K} \frac{1}{\sqrt{p}} h_{uv}^{(k)} \mathbf{c}_k b_u^{(k)}[0] + \mathbf{n}_{uv}, \quad p = 1, 2, \ldots, p, \quad u = 1, 2, \ldots, q. \tag{7}$$

Let us define

$$\begin{aligned}
\mathbf{y}_u &= \left[\mathbf{y}_{u1}^T, \mathbf{y}_{u2}^T, \ldots, \mathbf{y}_{up}^T\right]^T,\\
\mathbf{n}_u &= \left[\mathbf{n}_{u1}^T, \mathbf{n}_{u2}^T, \ldots, \mathbf{n}_{up}^T\right]^T,\\
\mathbf{h}_{ku} &= \frac{1}{\sqrt{p}}\left[h_{u1}^{(k)}, h_{u2}^{(k)}, \ldots, h_{up}^{(k)}\right]^T.
\end{aligned} \tag{8}$$

Then, $\mathbf{y}_u$ can be expressed as

$$\mathbf{y}_u = \sum_{k=1}^{K} \left(\mathbf{h}_{ku} \otimes \mathbf{c}_k\right) b_u^{(k)} + \mathbf{n}_u, \quad u = 1, 2, \ldots, q, \tag{9}$$

where $\otimes$ represents the *Kronecker product* [23] operation.

Furthermore, if we define

$$\begin{aligned}
\mathbf{b}_u &= \left[b_u^{(1)}[0], b_u^{(2)}[0], \ldots, b_u^{(K)}[0]\right]^T,\\
\mathbf{C} &= \left[\mathbf{c}_1, \mathbf{c}_2, \ldots, \mathbf{c}_K\right],\\
\mathbf{H}_u &= \left[\mathbf{h}_{1u}, \mathbf{h}_{2u}, \ldots, \mathbf{h}_{Ku}\right].
\end{aligned} \tag{10}$$

Then, (9) can alternatively be represented as

$$\mathbf{y}_u = \left(\mathbf{H}_u \square \mathbf{C}\right)\mathbf{b}_u + \mathbf{n}_u, \quad u = 1, 2, \ldots, q, \tag{11}$$

where $(\mathbf{H}_u \square \mathbf{C})$ represents the *Khatri-Rao product* between $\mathbf{H}_u$ and $\mathbf{C}$.

In summary, in (11) $\mathbf{y}_u$ is a pN_e-length observation vector, $\mathbf{H}_u$ is a $(p \times K)$-dimensional matrix due to the fading channels experienced by the subcarrier signals of the K users, $\mathbf{C}$ is a $(N_e \times K)$ matrix contributed by the spreading sequences of the K users, $\mathbf{b}_u$ contains K binary bits to be detected and, finally, $\mathbf{n}_u$ is the pN_e-length Gaussian noise vector distributed associated with mean zero and a covariance matrix of $\sigma^2\mathbf{I}_{pN_e}$, where $\mathbf{I}_{pN_e}$ is a $(pN_e \times pN_e)$ identity matrix.

Additionally, it can be shown that (7) can also be written as

$$\mathbf{y}_{uv} = \mathbf{C}\mathbf{H}_{uv}\mathbf{b}_u + \mathbf{n}_{uv}, \quad v = 1, 2, \ldots, p, \; u = 1, 2, \ldots, q, \tag{12}$$

where $\mathbf{H}_{uv}$ is a diagonal matrix expressed as

$$\mathbf{H}_{uv} = \frac{1}{\sqrt{p}}\mathrm{diag}\left\{h_{uv}^{(1)}, h_{uv}^{(2)}, \ldots, h_{uv}^{(K)}\right\}. \tag{13}$$

As shown in (11), the spreading code matrix $\mathbf{C}$ is certain once the users' spreading codes are given. The matrix $\mathbf{H}_u$ denoting the CIRs is known, once the channels are estimated. Let us now consider the multiuser detection in the MC DS-CDMA, which are derived based on (9), (11), or (12).

3. ZERO-FORCING MULTIUSER DETECTION

In this section, we consider the ZF-MUDs in the MC DS-CDMA system. These ZF-MUDs are capable of removing fully the MUI at the cost of enhancing the background noise [24]. We assume for ZF-MUD that the BS receiver employs the knowledge about $\mathbf{C}$ and $\mathbf{H}_u$. Let us consider first the optimum ZF-MUD, that is, the OZF-MUD.

3.1. Optimum zero-forcing multiuser detection

The OZF-MUD is derived based on (11) by jointly treating the observations without regarding to the specific subcarriers. The OZF-MUD is capable of achieving a better BER

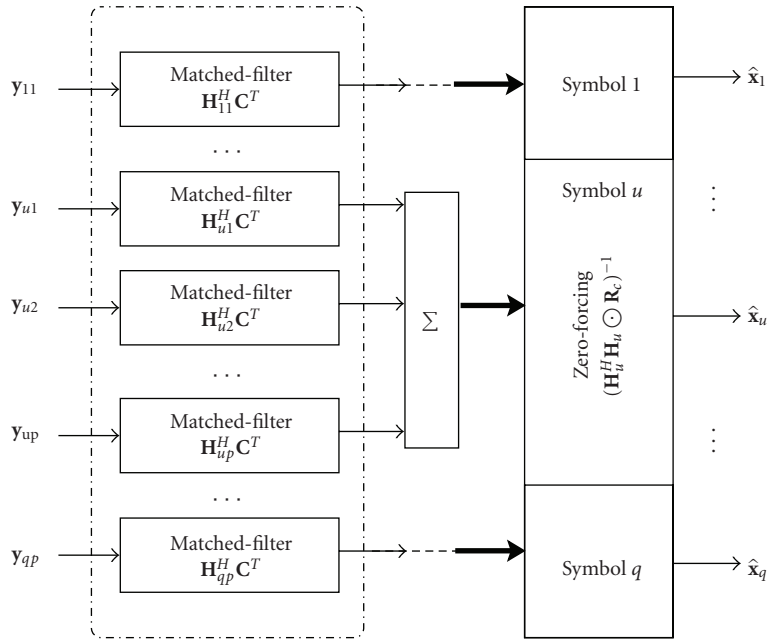

FIGURE 3: Schematic block diagram for implementation of the OZF-MUD in MC DS-CDMA systems.

performance than the SZF-MUD that will be derived later in Section3.2. However, its implementational complexity is much higher than that of the SZF-MUD.

The decision variable vector for $\mathbf{b}_u$ in the context of the OZF-MUD can be expressed as

$$\mathbf{z}_u = \mathbf{W}_u^H \mathbf{y}_u, \quad u = 1, 2, \ldots, q, \tag{14}$$

where, according to (11), it can be readily shown that the weight matrix $\mathbf{W}_u$ in ZF sense can be denoted as

$$\mathbf{W}_u = (\mathbf{H}_u \square \mathbf{C}) \left[(\mathbf{H}_u \square \mathbf{C})^H (\mathbf{H}_u \square \mathbf{C}) \right]^{-1}. \tag{15}$$

Using the property of $(\mathbf{H}_u \square \mathbf{C})^H (\mathbf{H}_u \square \mathbf{C}) = (\mathbf{H}_u^H \mathbf{H}_u \odot \mathbf{C}^T \mathbf{C})$ [23], where $\odot$ represents the *Hadamard product* operation [25], the above equation can be denoted as

$$\mathbf{W}_u = (\mathbf{H}_u \square \mathbf{C}) \left[(\mathbf{H}_u^H \mathbf{H}_u \odot \mathbf{R}_c) \right]^{-1}, \tag{16}$$

where $\mathbf{R}_c = \mathbf{C}^T \mathbf{C}$.

In (16), the matrix required to be inverted, that is, $(\mathbf{H}_u^H \mathbf{H}_u \odot \mathbf{R}_c)$, is a $(K \times K)$ matrix, which may be efficiently computed due to the following reasons. Firstly, $\mathbf{R}_c$ is a $(K \times K)$ time-invariant matrix, which can be computed once for all. Secondly, although $\mathbf{H}_u^H \mathbf{H}_u$ is a $(K \times K)$ time-variant matrix, it is only required to be updated at the level of fading rate of the wireless channels experienced by the subcarrier signals. Finally, the Hadamard product between $\mathbf{H}_u^H \mathbf{H}_u$ and $\mathbf{R}_c$ constitutes K^2 straightforward complex multiplications.

Upon applying (16) into (14), the decision variable vector can be written as

$$\mathbf{z}_u = \left[(\mathbf{H}_u^H \mathbf{H}_u \odot \mathbf{R}_c) \right]^{-1} (\mathbf{H}_u \square \mathbf{C})^H \mathbf{y}_u. \tag{17}$$

In (17), $(\mathbf{H}_u \square \mathbf{C})^H \mathbf{y}_u$ can be expressed as

$$\begin{aligned} (\mathbf{H}_u \square \mathbf{C})^H \mathbf{y}_u &= \left[\mathbf{h}_{1u} \otimes \mathbf{c}_1 \,|\, \mathbf{h}_{2u} \otimes \mathbf{c}_2 \,|\, \cdots \mathbf{h}_{Ku} \otimes \mathbf{c}_K \right]^H \begin{bmatrix} \mathbf{y}_{u1} \\ \mathbf{y}_{u2} \\ \vdots \\ \mathbf{y}_{up} \end{bmatrix} \\ &= \sum_{v=1}^{p} \mathbf{H}_{uv}^H \mathbf{C}^T \mathbf{y}_{uv}, \end{aligned} \tag{18}$$

where $\mathbf{H}_{uv}$ has been defined in (13) and $\mathbf{y}_{uv}$ is given by (12). Therefore, when substituting (18) into (17), we obtain

$$\mathbf{z}_u = \left[(\mathbf{H}_u^H \mathbf{H}_u \odot \mathbf{R}_c) \right]^{-1} \left(\sum_{v=1}^{p} \mathbf{H}_{uv}^H \mathbf{C}^T \mathbf{y}_{uv} \right), \quad u = 1, 2, \ldots, q. \tag{19}$$

Equation (19) shows that the OZF-MUD for $\mathbf{b}_u$ can be divided into p MF operations corresponding to the p number of subcarriers conveying $\mathbf{b}_u$ and one ZF operation, which multiplies a $(K \times K)$ matrix of $\left[(\mathbf{H}_u^H \mathbf{H}_u \odot \mathbf{R}_c) \right]^{-1}$ on the MFs' outputs. In summary, the OZF-MUD can be implemented by the schematic block diagram as shown in Figure 3.

3.2. Suboptimum zero-forcing multiuser detection

In the considered MC DS-CDMA, each subcarrier signal is constituted by K DS-CDMA signals belonging to K users and a data bit of a given user is conveyed by p subcarriers. In this type of MC DS-CDMA, the linear MUD may be implemented first by carrying out the MUD associated with each of the subcarriers. After the MUD at the subcarrier level, the subcarrier signals conveying the same data bit are coherently

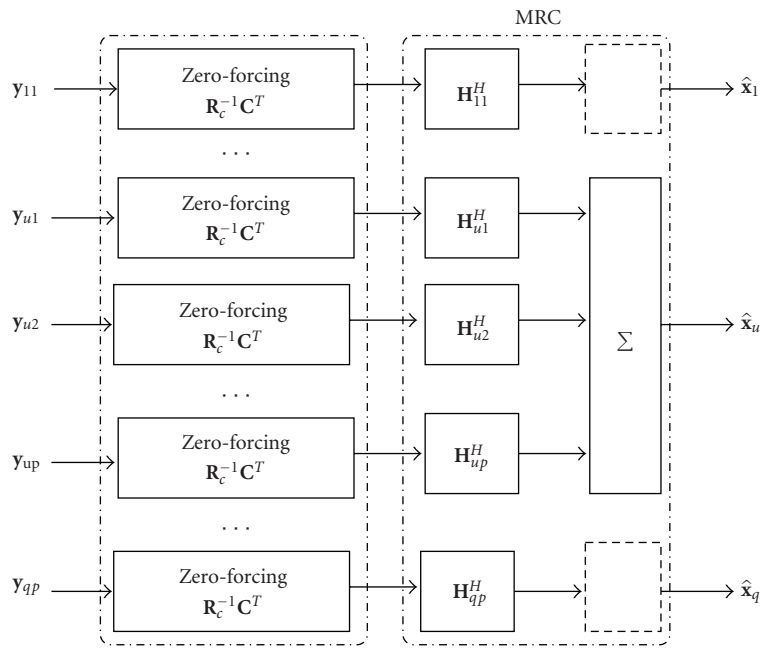

Figure 4: Schematic block diagram for implementation of the SZF-MUD in MC DS-CDMA systems.

combined in order to form a final decision variable. Specifically, when the SZF-MUD following this design philosophy is considered, for the uth data vector $\mathbf{b}_u$ transmitted by the K users, the decision variable vector in the context of the uvth subcarrier can be formed as

$$\mathbf{z}_{uv} = \mathbf{W}_{uv}^H \mathbf{y}_{uv}, \quad u = 1, 2, \ldots, q;\ v = 1, 2, \ldots, p, \tag{20}$$

where $\mathbf{W}_{uv}$ is a $(N_e \times K)$ weight matrix for processing the observation vector $\mathbf{y}_{uv}$ of (12). After the MUD operation of (20), the p subcarrier signals conveying $\mathbf{b}_u$ are then coherently combined to form the final decision variable, which can be expressed as

$$\mathbf{z}_u = \sum_{v=1}^{p} \mathbf{T}_{uv}^H \mathbf{z}_{uv}, \quad u = 1, 2, \ldots, q, \tag{21}$$

where the matrix $\mathbf{T}_{uv}$ is a postprocessing matrix carrying out the coherent combining, such as the maximal ratio combining (MRC).

It can be shown that, for the SZF-MUD using MRC, the weight matrix in ZF sense and the postprocessing matrix can be chosen as

$$\mathbf{W}_{uv} = \mathbf{C}\left(\mathbf{C}^T\mathbf{C}\right)^{-1} = \mathbf{C}\mathbf{R}_c^{-1}, \qquad \mathbf{T}_{uv} = \mathbf{H}_{uv}. \tag{22}$$

Upon substituting (12), (20), and (22) into (21), the decision variable vector for $\mathbf{b}_u$ can be expressed as

$$\begin{aligned} \mathbf{z}_u &= \sum_{v=1}^{p} \mathbf{T}_{uv}^H \mathbf{R}_c^{-1} \mathbf{C}^T \mathbf{y}_{uv} \\ &= \sum_{v=1}^{p} \mathbf{H}_{uv}^H \mathbf{H}_{uv} \mathbf{b}_u + \sum_{v=1}^{p} \mathbf{H}_{uv}^H \mathbf{R}_c^{-1} \mathbf{C}^T \mathbf{n}_{uv}, \quad u = 1, 2, \ldots, q. \end{aligned} \tag{23}$$

Note that since $\mathbf{H}_{uv}$ defined in (13) is a diagonal matrix, explicitly, the SZF-MUD is capable of removing fully the MUI and achieving a F domain diversity order of p.

In summary, the SZF-MUD can be implemented by the schematic block diagram of Figure 4. As shown in (22) and Figure 4, the weight matrix $\mathbf{W}_{uv}$ for the SZF-MUD is time-invariant and is common to any of the qp subcarriers. Hence, it can be computed "once for all," provided that the active users maintain unchanged. In this case, the proposed SZF-MUD having the processing matrices in (22) in fact has an implementational complexity that is similar to the single-user MF receiver. However, if the state of the active users changes rapidly, the weight matrix $\mathbf{W}_{uv}$ for the SZF-MUD is also required to be updated correspondingly. In this scenario, the proposed SZF-MUD having the processing matrices in (22) will have a higher complexity than the single-user MF receiver. Furthermore, when comparing Figure 4 with Figure 3, we can see that the time-variant channel matrices are invoked in the inverse operations in Figure 3 for the OZF-MUD, but not invoked in the inverse operations in Figure 4 for the SZF-MUD. In Figure 4 the channel-dependent time-variant matrices are only invoked in the linear processing as in the single-user MF-based receiver. Hence, we may be implied that the SZF-MUD will be more robust than the OZF-MUD to the channel estimation errors. However, as our simulation results in Section 6 shown, the error performance of the MC DS-CDMA using the SZF-MUD is much worse than that of the MC DS-CDMA using the OZF-MUD.

Figures 3 and 4 show that both the OZF-MUD and SZF-MUD have the modular structures. In Figure 3 the operations in the MF modular components are subcarrier-by-subcarrier independent. The ZF operations for the q bits of a user are bit-by-bit independent but subcarrier-by-subcarrier dependent for a given bit. By contrast, in Figure 4 the ZF

operations are subcarrier-by-subcarrier independent. Except the sum operation, the MRC operations are also subcarrier-by-subcarrier independent. Explicitly, the modular structures of the OZF-MUD and SZF-MUD as shown in Figures 3 and 4 are beneficial to implementation and reconfiguration in practice. For example, in a dynamic communications environment such as in cognitive radio, when certain frequency bands are occupied and some of the subcarriers in the MC DS-CDMA are sensed having high interference temperature, the OZF-MUD in Figure 3 and the SZF-MUD in Figure 4 can be correspondingly reconfigured in order to adapt to the changed environment. Specifically, for the OZF-MUD as shown in Figure 3, the subcarrier branches having the high interference temperature can be directly deleted from the receiver. However, the matrices implementing the ZF operations must be updated by removing the CIRs corresponding to the subcarriers having the high interference temperature. By contrast, the SZF-MUD as shown in Figure 4 can be updated simply by deleting the subcarrier branches having the high interference temperature, that is, by setting the corresponding observation vectors in the form of $\mathbf{y}_{uv}$ to the zero vectors.

3.3. Interference cancellation aided suboptimum zero-forcing

The error performance of the MC DS-CDMA using the SZF-MUD may be significantly enhanced by employing a stage of IC following the SZF-MUD, yielding the SZF-IC. Our simulation results in Section 6 show that the MC DS-CDMA using SZF-IC is capable of achieving the near single-user BER performance. Furthermore, since the channel-dependent operations at the IC stage are also linear operations, we can be implied that the SZF-IC should be similarly robust as the SZF-MUD to the channel estimation errors.

The SZF-IC can be operated as the following steps.

Step 1. SZF-MUD operation generates the decision variable vector $\mathbf{z}_u (u = 1, 2, \ldots, q)$ as shown in (23).

Step 2. Based on $\mathbf{z}_u (u = 1, 2, \ldots, q)$, make decisions as

$$\hat{\mathbf{b}}_u = \operatorname{sign}(\mathbf{z}_u), \quad u = 1, 2, \ldots, q, \tag{24}$$

where $\operatorname{sign}(x)$ is a sign-function.

Step 3. For $k = 1, 2, \ldots, K$, the IC is carried out, yielding

$$\mathbf{y}_{uv}^{(k)} = \mathbf{y}_{uv} - \mathbf{C}\mathbf{H}_{uv}\hat{\mathbf{b}}_u\left(\hat{b}_u^{(k)} = 0\right), \tag{25}$$

where $\hat{\mathbf{b}}_u(\hat{b}_u^{(k)} = 0)$ is the result after setting $\hat{b}_u^{(k)} = 0$ in $\hat{\mathbf{b}}_u$.

Step 4. Forming the decision variable again for $b_u^{(k)}$ as

$$\hat{z}_u^{(k)} = \frac{1}{\sqrt{p}} \sum_{v=1}^{p} \left(h_{uv}^{(k)}\right)^* \mathbf{c}_k^T \mathbf{y}_{uv}^{(k)}, \quad u = 1, 2, \ldots, q;\ k = 1, 2, \ldots, K \tag{26}$$

and the decision for $b_u^{(k)}$ is finally made according to $\tilde{b}_u^{(k)} = \operatorname{sign}(\hat{z}_u^{(k)})$.

Having derived various ZF-MUDs in this section, let us now turn to consider the MMSE-MUDs.

4. MMSE MULTIUSER DETECTION

In this section, the MMSE-MUDs for detection of the MC DS-CDMA signals are derived. Specifically, one optimum MMSE-MUD (OMMSE-MUD), two suboptimum MMSE-MUDs (SMMSE-MUDs) and one IC-aided SMMSE-MUD, that is, SMMSE-IC, are considered. It can be shown that these MMSE-MUDs are capable of mitigating efficiently the MUI while suppressing the background noise. Let us first consider the OMMSE-MUD.

4.1. Optimum MMSE multiuser detection

The OMMSE-MUD is derived based on (11) and it jointly processes the observations without regarding to the specific subcarriers. The OMMSE-MUD is capable of achieving a better BER performance than both the SMMSE-MUDs, which will be derived in Sections 4.2 and 4.3.

The decision variable vector for the OMMSE-MUD can be expressed as

$$\mathbf{z}_u = \mathbf{W}_u^H \mathbf{y}_u, \quad u = 1, 2, \ldots, q, \tag{27}$$

where the optimum weight matrix in MMSE sense can be expressed as

$$\mathbf{W}_u = \mathbf{R}_{\mathbf{y}_u}^{-1} \mathbf{R}_{\mathbf{y}_u \mathbf{b}_u} \tag{28}$$

with $\mathbf{R}_{\mathbf{y}_u}$ being a $(pN_e \times pN_e)$ auto-correlation matrix of $\mathbf{y}_u$, which, according to (11), is given by

$$\mathbf{R}_{\mathbf{y}_u} = (\mathbf{H}_u \square \mathbf{C})(\mathbf{H}_u \square \mathbf{C})^H + \sigma^2 \mathbf{I}_{pN_e}. \tag{29}$$

In (28), $\mathbf{R}_{\mathbf{y}_u \mathbf{b}_u}$ is the cross-correlation matrix between $\mathbf{y}_u$ and $\mathbf{b}_u$, which can be expressed as

$$\mathbf{R}_{\mathbf{y}_u \mathbf{b}_u} = (\mathbf{H}_u \square \mathbf{C}) \tag{30}$$

which is a $(pN_e \times K)$ matrix. After substituting (29) and (30) into (28), the weight matrix in the context of the OMMSE-MUD can be expressed as

$$\mathbf{W}_u = \left[(\mathbf{H}_u \square \mathbf{C})(\mathbf{H}_u \square \mathbf{C})^H + \sigma^2 \mathbf{I}_{pN_e}\right]^{-1} (\mathbf{H}_u \square \mathbf{C}), \quad u = 1, 2, \ldots, q. \tag{31}$$

Therefore, when the receiver employs no knowledge about the interfering users including their signature sequences and CIRs, except for the desired user, the receiver has to invert a matrix of size $(pN_e \times pN_e)$-dimensional, as seen in (31). In this case, the complexity of the OMMSE-MUD might be extreme, when the product of pN_e is high.

By contrast, when the receiver has the knowledge about all the K active users, all the K users can be detected simultaneously. In this case, when invoking the *matrix inverse lemma* on (31), we obtain

$$\begin{aligned} \mathbf{W}_u &= (\mathbf{H}_u \square \mathbf{C})\left[(\mathbf{H}_u \square \mathbf{C})^H (\mathbf{H}_u \square \mathbf{C}) + \sigma^2 \mathbf{I}_K\right]^{-1} \\ &= (\mathbf{H}_u \square \mathbf{C})\left[(\mathbf{H}_u^H \mathbf{H}_u \odot \mathbf{R}_c) + \sigma^2 \mathbf{I}_K\right]^{-1}, \quad u = 1, 2, \ldots, q \end{aligned} \tag{32}$$

which shows that the OMMSE-MUD is only required to invert a $(K \times K)$ matrix.

Finally, upon substituting (32) into (27) and following the steps from (17) to (19), the decision variable vector in the context of the OMMSE-MUD can be represented as

$$\mathbf{z}_u = \left[\left(\mathbf{H}_u^H \mathbf{H}_u \odot \mathbf{R}_c\right) + \sigma^2 \mathbf{I}_K\right]^{-1} \left(\sum_{v=1}^{p} \mathbf{H}_{uv}^H \mathbf{C}^T \mathbf{y}_{uv}\right), \quad u = 1, 2, \ldots, q. \tag{33}$$

Equation (33) shows that, when the receiver employs the knowledge about all the K active users, the OMMSE-MUD can be implemented by two stages: the first-stage implements the correlation operation in the context of each of the subcarriers. By contrast, the second-stage carries out a MMSE-based interference suppression in order to mitigate the MUI. The complexity of the OMMSE-MUD represented by (33) is dominated by the inverse of a $(K \times K)$ matrix as seen in (33).

The OMMSE-MUD of (33) can be implemented by the schematic block diagram as shown in Figure 3, which is for the OZF-MUD. For the OMMSE-MUD, the ZF operation of $\left(\mathbf{H}_u^H \mathbf{H}_u \odot \mathbf{R}_c\right)^{-1}$ in Figure 3 should be replaced by the MMSE-based operation of $\left[\left(\mathbf{H}_u^H \mathbf{H}_u \odot \mathbf{R}_c\right) + \sigma^2 \mathbf{I}_K\right]^{-1}$. Let us now consider the SMMSE-MUDs.

4.2. Suboptimum MMSE multiuser detection: type I

As the SZF-MUD derived in Section 3.2, the MMSE-MUD can also be implemented first in the context of each of the qp subcarriers, and then by combining the signals across the subcarriers conveying the same data bits of the K users. This type of MMSE-MUDs forms the class of suboptimum MMSE-MUDs (SMMSE-MUDs). Below two SMMSE-MUD schemes are derived, namely SMMSE-MUD-I and SMMSE-MUD-II. In this subsection, we consider the SMMSE-MUD-I, while the SMMSE-MUD-II is discussed in Section 4.3.

In the context of the SMMSE-MUD-I, when the MMSE detection principle is applied for each of the subcarriers, the decision variable vector for $\mathbf{x}_u$ can be expressed as

$$\mathbf{z}_u = \sum_{v=1}^{p} \mathbf{W}_{uv}^H \mathbf{y}_{uv}, \quad u = 1, 2, \ldots, q, \tag{34}$$

where $\mathbf{y}_{uv}$ is the observation vector from the uvth subcarrier, which is given by (12), and $\mathbf{W}_{uv}$ is the optimum weight matrix for the uvth subcarrier, which can be expressed as

$$\mathbf{W}_{uv} = \mathbf{R}_{\mathbf{y}_{uv}}^{-1} \mathbf{R}_{\mathbf{y}_{uv}\mathbf{b}_u}, \tag{35}$$

where $\mathbf{R}_{\mathbf{y}_{uv}}$ represents the autocorrelation matrix of $\mathbf{y}_{uv}$, while $\mathbf{R}_{\mathbf{y}_{uv}\mathbf{b}_u}$ represents the cross-correlation matrix between $\mathbf{y}_{uv}$ and $\mathbf{b}_u$. With the aid of (12), it can be readily shown that

$$\mathbf{R}_{\mathbf{y}_{uv}} = \mathbf{C}\mathbf{H}_{uv} \mathbf{H}_{uv}^H \mathbf{C}^T + \sigma^2 \mathbf{I}_{N_e}, \tag{36}$$

$$\mathbf{R}_{\mathbf{y}_{uv}\mathbf{b}_u} = \mathbf{C}\mathbf{H}_{uv}. \tag{37}$$

Consequently, when substituting (36) and (37) into (35), the optimum weight matrix $\mathbf{W}_{uv}$ corresponding to the uvth subcarrier can be expressed as

$$\mathbf{W}_{uv} = \left(\mathbf{C}\mathbf{H}_{uv} \mathbf{H}_{uv}^H \mathbf{C}^T + \sigma^2 \mathbf{I}_{N_e}\right)^{-1} \mathbf{C}\mathbf{H}_{uv}, \quad u = 1, 2, \ldots, q \tag{38}$$

which includes the inverse of a $(N_e \times N_e)$ matrix.

The SMMSE-MUD-I having the weight matrix of (38) does not require the knowledge about the interfering users, since the autocorrelation matrix $\mathbf{R}_{\mathbf{y}_{uv}}$ in (36) and the cross-correlation matrix $\mathbf{R}_{\mathbf{y}_{uv}\mathbf{b}_u}$ in (37) may be estimated from the observations obtained at the uvth subcarrier. It can also be implemented adaptively or even blindly [20]. However, when the receiver employs the knowledge about the interfering users, the *matrix inverse lemma* can be invoked, which can modify the weight matrix of (38) to

$$\mathbf{W}_{uv} = \mathbf{C}\mathbf{H}_{uv} \left(\mathbf{H}_{uv}^H \mathbf{C}^T \mathbf{C}\mathbf{H}_{uv} + \sigma^2 \mathbf{I}_K\right)^{-1}, \quad u = 1, 2, \ldots, q. \tag{39}$$

In this case the SMMSE-MUD-I is required to invert a $(K \times K)$ matrix for each of the pq subcarriers.

Finally, when substituting (12) and (39) into (34), the decision variable vector for the SMMSE-MUD-I can be expressed as

$$\mathbf{z}_u = \sum_{v=1}^{p} \left[\mathbf{I}_K - \left(\mathbf{H}_{uv}^H \mathbf{C}^T \mathbf{C}\mathbf{H}_{uv} + \sigma^2 \mathbf{I}_K\right)^{-1}\right] \mathbf{b}_u + \sum_{v=1}^{p} \left(\mathbf{H}_{uv}^H \mathbf{C}^T \mathbf{C}\mathbf{H}_{uv} + \sigma^2 \mathbf{I}_K\right)^{-1} \mathbf{H}_{uv}^H \mathbf{C}^T \mathbf{n}_{uv}, \quad u = 1, 2, \ldots, q. \tag{40}$$

When comparing the weight matrix of (32) for the OMMSE-MUD and the weight matrix of (39) for the SMMSE-MUD-I, it can be known that the SMMSE-MUD-I may have a complexity, which is even higher than that of the OMMSE-MUD. As seen in (32), the OMMSE-MUD only needs to invert a $(K \times K)$ matrix in order to detect $\mathbf{b}_u$. By contrast, as shown in (39), the SMMSE-MUD-I has to invert p matrices of size $(K \times K)$. Furthermore, our simulation results in Section 6 show that the BER performance of the SMMSE-MUD-I is worse than that of the OMMSE-MUD.

As shown in (36) the autocorrelation matrix $\mathbf{R}_{\mathbf{y}_{uv}}$ in the SMMSE-MUD-I is time-variant, it should be estimated within a time-duration when the corresponding channels retain unchanged. Hence, the average taken for estimating $\mathbf{R}_{\mathbf{y}_{uv}}$ as shown in (36) is a short-term average. Instead, the autocorrelation matrix $\mathbf{R}_{\mathbf{y}_{uv}}$ may be estimated using the long-term average, yielding the SMMSE-MUD-II, which is now discussed in the next subsection.

4.3. Suboptimum MMSE multiuser detection type II

It is well known that the single-user MF-assisted detector is much more robust to the channel estimation errors, in comparison with various types of multiuser detectors [26, 27].

Hence, in MUD design it is often preferable to include a relatively lower number of channel-dependent operations, especially, the channel-dependent matrix-inverse operation. Furthermore, from (38) and (39) we can be implied that the high-complexity of the SMMSE-MUD-I is mainly because the matrices need to be inverted are time-variant due to using the short-term average. When the long-term average is applied for estimating $\mathbf{R}_{\mathbf{y}_{uv}}$, we can obtain

$$\mathbf{R}_{\mathbf{y}_{uv}} = \frac{\Omega}{p}\mathbf{C}\mathbf{C}^T + \sigma^2\mathbf{I}_{N_e}, \tag{41}$$

where $\Omega = E[\|h_{uv}^{(k)}\|^2]$. In this case, when substituting (41) and (37) into (35), the optimum weight matrix in the SMMSE-MUD-II can be expressed as

$$\begin{aligned}\mathbf{W}_{uv} &= p\left(\Omega\mathbf{C}\mathbf{C}^T + p\sigma^2\mathbf{I}_N\right)^{-1}\mathbf{C}\mathbf{H}_{uv} \\ &= p\mathbf{C}\left(\Omega\mathbf{R}_c + p\sigma^2\mathbf{I}_K\right)^{-1}\mathbf{H}_{uv} \\ &\triangleq \mathbf{C}\left(\Omega\mathbf{R}_c + p\sigma^2\mathbf{I}_K\right)^{-1}\mathbf{H}_{uv}, \quad u = 1, 2, \ldots, q.\end{aligned} \tag{42}$$

Consequently, the decision variable vector $\mathbf{z}_u$ can be expressed as

$$\mathbf{z}_u = \sum_{v=1}^{p}\mathbf{H}_{uv}^H\left(\Omega\mathbf{R}_c + p\sigma^2\mathbf{I}_K\right)^{-1}\mathbf{C}^T\mathbf{y}_{uv}, \quad u = 1, 2, \ldots, q. \tag{43}$$

From (43) we can observe that in the SMMSE-MUD-II the matrices required to be inverted are time-invariant, and the MRC is achieved through multiplying the ZF-MUD's output with the channel-dependent matrix $\mathbf{H}_{uv}^H$. Since only the MRC operation invokes the time-variant CIR matrices, the SMMSE-MUD-II hence should have the same robustness to the channel estimation errors as the single-user MF detector. Furthermore, in (43) the matrices need to be inverted are only required to compute once, provided that the active users maintain unchanged. Therefore, the SMMSE-MUD-II can be implemented with a complexity that is also similar to that of the single-user MF detector.

The schematic block diagram for the SMMSE-MUD-II can be represented by Figure 4, which is for the SZF-MUD, after replacing the ZF-operation of $\mathbf{R}_c^{-1}\mathbf{C}^T$ by the MMSE-related operation of $\left(\Omega\mathbf{R}_c + p\sigma^2\mathbf{I}_K\right)^{-1}\mathbf{C}^T$.

Above three types of MMSE-MUDs have been derived. As our simulation results in Section 6 shown, the SMMSE-MUD-II achieves the worst BER performance among these MMSE-MUDs. However, the BER performance of the SMMSE-MUD-II can be significantly improved, when a stage of IC is employed following the SMMSE-MUD-II detection, yielding the so-called SMMSE-IC. Specifically, the SMMSE-IC can be implemented in the same way as the SZF-IC—which has been discussed in Section 3.3—by replacing the first-stage of ZF detection in the SZF-IC by a first-stage of SMMSE-MUD-II assisted detection for the SMMSE-IC. Therefore, the algorithm for the SMMSE-IC is not stated here in detail.

5. IMPLEMENTATION CONSIDERATION

According to our analysis in Sections 3 and 4, we can find that all the proposed MUD schemes, which include OZF-MUD, SZF-MUD and SZF-IC in the ZF family as well as OMMSE-MUD, SMMSE-MUT-I, SMMSE-MUD-II and SMMSE-IC in the MMSE family, can be implemented in modular structures, such as, shown in Figures 3 and 4. As we mentioned previously, the modular structures of the MUDs are beneficial to implementation and reconfiguration in practice, especially, when dynamic communications environments such as cognitive radios are considered. In cognitive radios the communications environments might be highly dynamic, different frequency bands may experience different interference temperature, which itself may also be time-variant. In order to achieve high-efficiency communications in the dynamic communications environments, it is desirable that the transmission signalling as well as the detection algorithms can be reconfigured conveniently and also with a low impact on the overall system.

Due to the multi-band structure, MC DS-CDMA explicitly constitutes one of the signalling schemes that are well suitable for cognitive radios. In the MC DS-CDMA supported cognitive radios, when some frequency bands being used are sensed with high interference, their corresponding subcarriers may be turned off. By contrast, when some other frequency bands, which have not been used yet, are sensed with low interference, their corresponding subcarriers can be activated in order to improve the overall bandwidth efficiency of wireless communications.

Following the reconfiguration of the transmission frequency bands, the detection scheme in receiver is required to be reconfigured correspondingly, desirably, with low-complexity. From our analysis in Sections 3 and 4, it can be shown that the MUD schemes considered in this contribution, especially the SZF-MUD, SMMSE-MUD-II, SZF-IC, and SMMSE-IC schemes, constitute a range of promising MUD schemes for deployment in cognitive radios. Firstly, these MUD schemes are low-complexity MUD schemes operated in ZF, MMSE and interference cancellation principles. Secondly, these MUD schemes employ the modular structures that are beneficial to reconfiguration. Specifically, for the OZF-MUD shown in (19) (also see Figure 3) and the OMMSE-MUD in (33), since the correlation operations are subcarrier-by-subcarrier independent, the correlation operation in the context of a subcarrier can be readily added or removed, when the subcarrier is activated or deactivated. However, as shown in (19) and (33), both the OZF-MUD and OMMSE-MUD need to recompute the inverse matrix, once the channel states change. By contrast, for the SZF-MUD, SMMSE-MUD-II, SZF-IC and SMMSE-IC schemes, since all the operations are subcarrier-by-subcarrier independent, the operation in the context of a subcarrier can hence be readily added or removed without addressing any impact on the other subcarriers. Furthermore, as our simulation results in Section 6 shown, the SZF-IC and SMMSE-IC are capable of achieving a similar BER performance as the optimum MUD based on the maximum likelihood (ML) principles [24].

Table 1: Comparison of the OZF-MUD (19), SZF-MUD (23), and the SZF-IC in Section 3.3.

	OZF-MUD	SZF-MUD	SZF-IC
Complexity	$O(K^2)$	$O(N_e)$	$O(N_e)$
Error performance	Near-best	Worst	Best
Sensitivity to channel estimation error	High	Low	Low
Flexibility for adaptation	Low	High	High

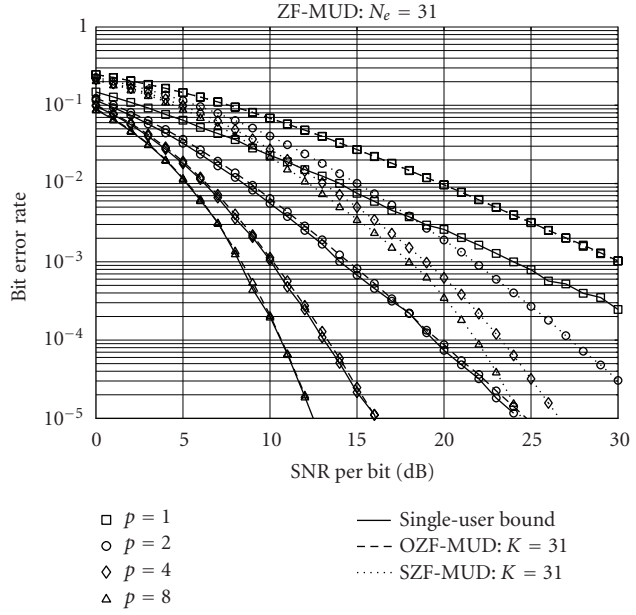

Figure 5: BER versus average SNR per bit performance for the MC DS-CDMA using Gold-sequences and having a T domain spreading factor of $N_e = 31$, when communicating over frequency-selective Rayleigh fading channels.

In summary, the comparison among the ZF-related MUDs is summarized in Table 1, while that among the MMSE-related MUDs is summarized in Table 2. Note that, in these tables the complexity denotes the complexity per symbol per user. For example, for the OZF-MUD and OMMSE-MUD as shown in (19) and (33), both of them need to compute the inverse of a time-variant $(K \times K)$ matrices, which has a complexity of $O(K^3)$, where $O(\cdot)$ means proportional to. Therefore, the complexity per symbol per user is of order $O(K^3/K) = O(K^2)$. By contrast, for the SZF-MUD of (23), SZF-IC in Section 3.3, SMMSE-MUD-I of (43) and SMMSE-IC in Section 4.3, since the inverse matrices are time-invariant, the highest complexity comes from the multiplication of a $(K \times N_e)$ matrix with a N_e-length vector, that is, from $\mathbf{C}^T\mathbf{y}_{uv}$. Hence, when the number of multiplications is counted, the complexity per symbol per user is of order $O(KN_e/K) = O(N_e)$.

Let us now illustrate a range of performance results for all the MUD schemes considered in this contribution.

6. PERFORMANCE RESULTS

In this section, we show a range of BER performance results for the MC DS-CDMA systems using the MUD schemes considered in this contribution, when communicating over frequency-selective Rayleigh fading channels. For convenience, the parameters shown in the figures are summarized as follows:

(i) SNR per bit: signal-to-noise ratio (SNR) per bit;
(ii) N_e: T domain spreading factor per subcarrier;
(iii) p: number of subcarriers conveying a data bit;
(iv) K: number of users supported by the MC DS-CDMA.

In our simulations, the T domain spreading sequences were chosen from the family of Gold-sequences of length $N_e = 31$. Furthermore, for comparison, the single-user (BER) bound achieved by the corresponding MC DS-CDMA system supporting single user is also shown in the figures.

Figure 5 shows the BER performance of the MC DS-CDMA system using both the OZF-MUD and SZF-MUD and supporting $K = 31$ users, when communicating over frequence-selective fading channels. From the results of Figure 5 we can observe that, when the Gold-sequences are employed for spreading, the OZF-MUD is capable of achieving the near single-user BER performance, when the number of subcarriers conveying a data bit is $p = 2, 4$, or 8, or when the F-domain diversity order is $p = 2, 4$, and 8. However, when without using the F-domain diversity corresponding to $p = 1$, the OZF-MUD cannot achieve the near single-user BER performance. Instead, as shown in Figure 5, at the BER of 10^{-3} the BER performance of the OZF-MUD is more than 5 dB worse than the single-user BER performance. As shown in Figure 5, although the SZF-MUD does have the capability to suppress the MUI, its achievable BER performance is significantly worse than that achieved by the OZF-MUD, when the F-domain diversity order is higher than one. When $p = 1$ both the OZF-MUD and SZF-MUD achieve the same BER performance, since in this case the OZF-MUD is equivalent to the SZF-MUD.

The BER versus SNR per bit performance of the MC DS-CDMA using the SZF-IC is shown in Figure 6 in conjunction with the BER performance of using the SZF-MUD and the single-user BER bound. As shown in Figure 6, when a IC-stage is applied following the SZF-MUD, the near single-user BER performance can always be achievable regardless of the F domain diversity order, even when the MC DS-CDMA supports $K = N_e = 31$ users, that is, when the MC DS-CDMA is fully loaded.

The BER versus SNR per bit performance of the MC DS-CDMA employing various MMSE-MUDs is plotted in Figures 7 and 8, when communicating over frequency-selective Rayleigh fading channels yielding that the subcarrier channels conveying a data bit experience independent Rayleigh fading. Specifically, in Figure 7 the BER of the MC DS-CDMA employing the OMMSE-MUD, SMMSE-MUD-I as well as the single-user BER bound are plotted, when the F-domain diversity order is $p = 1, 2, 4, 8$, respectively. By contrast, in Figure 8 the BER performance of the MC DS-CDMA employing the SMMSE-MUD-I,

Table 2: Comparison of the SMMSE-MUD-I (39), SMMSE-MUD-II (42), and the OMMSE-MUD (32).

	OMMSE-MUD	SMMSE-MUD-I	SMMSE-MUD-II	SMMSE-IC
Complexity	$O(p^3N_e^3)/K$ (no CIRs), $O(K^2)$ (CIRs)	$O(pN_e^3)/K$ (no CIRs), $O(pK^2)$ (CIRs)	$O(N_e)$	$O(N_e)$
Error performance	Near-best	Medium	Worst	Best
Sensitivity to channel estimation error	High	High	Low	Low
Flexibility for adaptation	Low	Low	High	High

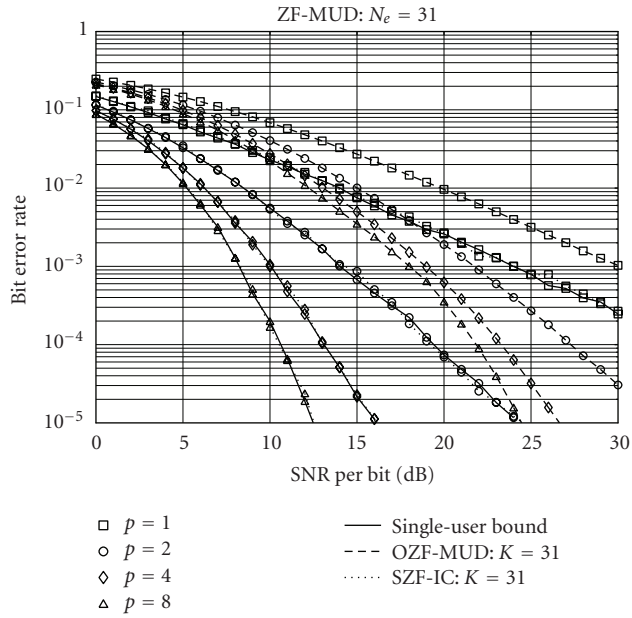

Figure 6: BER versus average SNR per bit performance for the MC DS-CDMA using Gold-sequences and having a T domain spreading factor of $N_e = 31$, when communicating over frequency-selective Rayleigh fading channels.

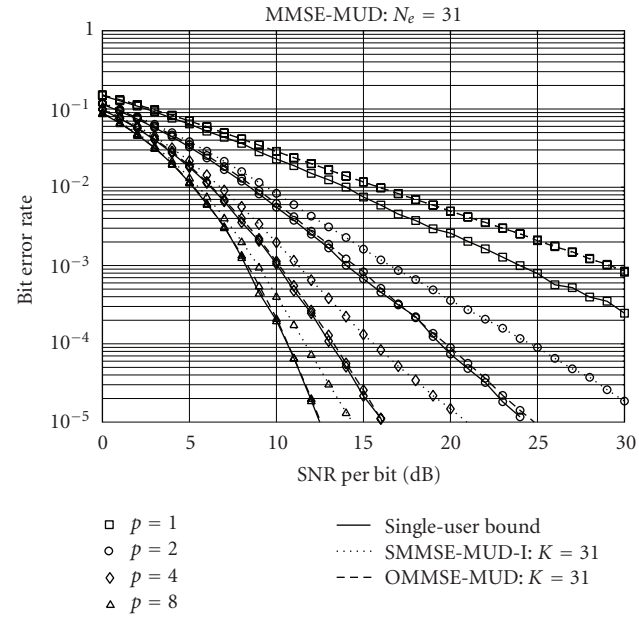

Figure 7: BER versus average SNR per bit performance for the MC DS-CDMA using Gold-sequences and having a T domain spreading factor of $N_e = 31$, when communicating over frequency-selective Rayleigh fading channels.

SMMSE-MUD-II as well as the single-user BER bound are considered, also when the F-domain diversity order is $p = 1, 2, 4, 8$, respectively. From the results of Figures 7 and 8, explicitly, the SMMSE-MUD-I outperforms the SMMSE-MUD-II, and the OMMSE-MUD outperforms both the SMMSE-MUD-I and SMMSE-MUD-II, when considering the achievable BER performance. As shown in Figure 7, the BER performance achieved by the OMMSE-MUD is very close to the single-user BER bound, when $p = 2, 3, 4$. By contrast, both the OMMSE-MUD and SMMSE-MUD-I achieve the same BER performance when $p = 1$. Furthermore, when $p = 1$, as shown in Figure 8, the BER performance of the SMMSE-MUD-II is slightly worse than that achieved by the SMMSE-MUD-I or by the OMMSE-MUD.

Finally, the BER performance of the SMMSE-IC is depicted in Figure 9 in conjunction with the BER of the corresponding SMMSE-MUD-II and the corresponding single-user BER bound. As can be seen in Figure 9, when an IC-stage is applied following the SMMSE-MUD-II detection, the MC DS-CDMA system is capable of achieving the near single-user BER performance.

In other words, the results of Figures 6 and 9 show that, when an IC-stage is employed after either the SZF-MUD or the SMMSE-MUD-II, the MC DS-CDMA system is capable of achieving a BER performance that is only achievable by the optimum MUD based on the ML principles [24]. However, as our analysis in Sections 3.3 and 4.3 shown, both the SZF-IC and SMMSE-IC have an implementational complexity that is significantly lower than that of the ML-aided MUD, whose complexity is exponentially proportional to the number of users [24].

7. CONCLUSIONS

In summary, in this contribution a range of low-complexity, high-flexibility, and robust MUD schemes have been derived for the MC DS-CDMA, which constitutes a multiple access scheme suitable for operation in dynamic communications environments. The MUD schemes have been derived based on the principles of ZF, MMSE and IC. The BER performance of the MC DS-CDMA in conjunction with the proposed MUD schemes has been investigated by simulations. It can be shown that all the MUD schemes are capable of

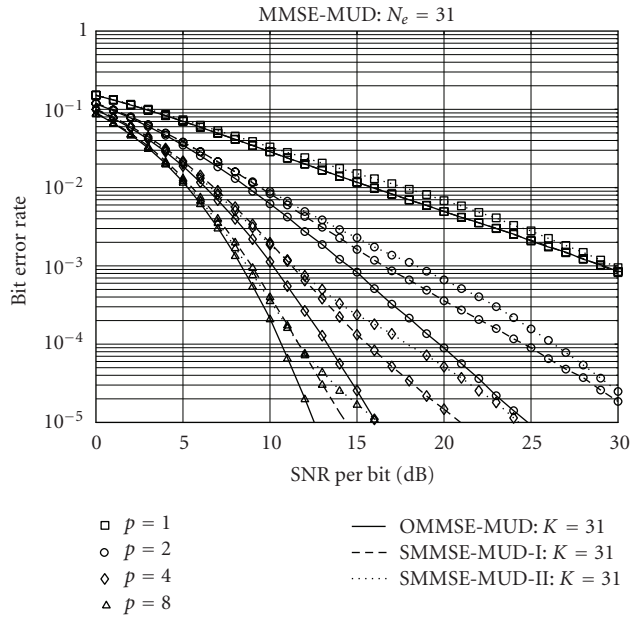

Figure 8: BER versus average SNR per bit performance for the MC DS-CDMA using Gold-sequences and having a T domain spreading factor of $N_e = 31$, when communicating over frequency-selective Rayleigh fading channels.

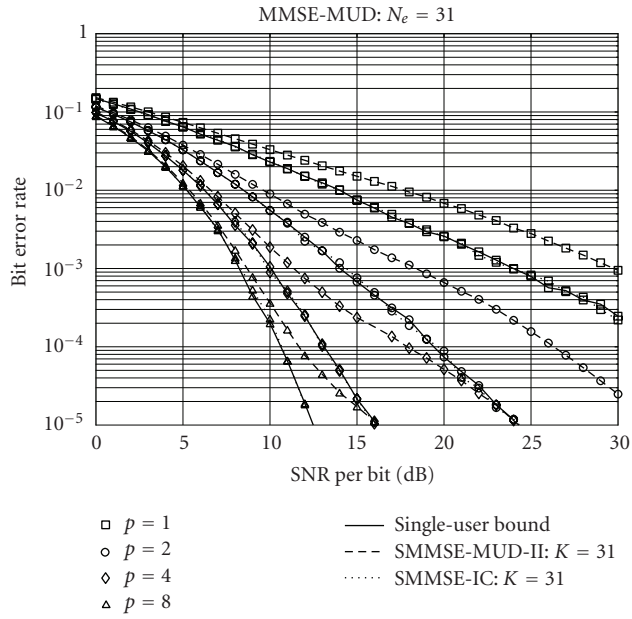

Figure 9: BER versus average SNR per bit performance for the MC DS-CDMA using Gold-sequences and having a T domain spreading factor of $N_e = 31$, when communicating over frequency-selective Rayleigh fading channels.

mitigating efficiently the MUI. Our study shows that the ZF-MUDs and MMSE-MUDs in MC DS-CDMA can usually be implemented using modular structures, where most modules are independent of each other. Moreover, our study shows that the SZF-MUD, SZF-IC, SMMSE-MUD-II, or SMMSE-IC has a fully subcarrier-by-subcarrier independent modular structure, where each of the modules may be reconfigured without effect on the others. Due to its high-flexibility for both transmission and detection, we may conclude that the MC DS-CDMA aided by a proposed high-flexibility MUD constitutes one of the promising candidates for dynamic communications environments such as in cognitive radios.

ACKNOWLEDGMENT

The author would like to acknowledge with thanks the financial assistance from EPSRC of UK.

REFERENCES

[1] J. Mitola III, "The software radio architecture," *IEEE Communications Magazine*, vol. 33, no. 5, pp. 26–38, 1995.

[2] J. Mitola III and G. Q. Maguire Jr., "Cognitive radio: making software radios more personal," *IEEE Personal Communications*, vol. 6, no. 4, pp. 13–18, 1999.

[3] S. Haykin, "Cognitive radio: brain-empowered wireless communications," *IEEE Journal on Selected Areas in Communications*, vol. 23, no. 2, pp. 201–220, 2005.

[4] N. Devroye, P. Mitran, and V. Tarokh, "Limits on communications in a cognitive radio channel," *IEEE Communications Magazine*, vol. 44, no. 6, pp. 44–49, 2006.

[5] L.-L. Yang and L. Hanzo, "Multicarrier DS-CDMA: a multiple access scheme for ubiquitous broadband wireless communications," *IEEE Communications Magazine*, vol. 41, no. 10, pp. 116–124, 2003.

[6] L.-L. Yang and L. Hanzo, "Performance of broadband multicarrier DS-CDMA using space-time spreading-assisted transmit diversity," *IEEE Transactions on Wireless Communications*, vol. 4, no. 3, pp. 885–894, 2005.

[7] S. Kondo and L. B. Milstein, "Performance of multicarrier DS CDMA systems," *IEEE Transactions on Communications*, vol. 44, no. 2, pp. 238–246, 1996.

[8] E. A. Sourour and M. Nakagawa, "Performance of orthogonal multicarrier CDMA in a multipath fading channel," *IEEE Transactions on Communications*, vol. 44, no. 3, pp. 356–367, 1996.

[9] G. Xiang and T. S. Ng, "Performance of asynchronous orthogonal multicarrier CDMA system in frequency selective fading channel," *IEEE Transactions on Communications*, vol. 47, no. 7, pp. 1084–1091, 1999.

[10] L.-C. Wang and C.-W. Chang, "On the performance of multicarrier DS-CDMA with imperfect power control and variable spreading factors," *IEEE Journal on Selected Areas in Communications*, vol. 24, no. 6, pp. 1154–1165, 2006.

[11] L.-L. Yang and L. Hanzo, "Performance of generalized multicarrier DS-CDMA over Nakagami-*m* fading channels," *IEEE Transactions on Communications*, vol. 50, no. 6, pp. 956–966, 2002.

[12] L.-L. Yang, "Time-hopping multicarrier code-division multiple access," *IEEE Transactions on Vehicular Technology*, vol. 56, no. 2, pp. 731–741, 2007.

[13] V. Tarokh, N. Seshadri, and A. R. Calderbank, "Space-time codes for high data rate wireless communication: performance criterion and code construction," *IEEE Transactions on Information Theory*, vol. 44, no. 2, pp. 744–765, 1998.

[14] I. E. Telatar, "Capacity of multiantenna Gaussian channels," *European Transactions on Telecommunications*, vol. 10, no. 6, pp. 585–595, 1999.

[15] L.-L. Yang and L. Hanzo, "Software-defined-radio-assisted adaptive broadband frequency hopping multicarrier DS-CDMA," *IEEE Communications Magazine*, vol. 40, no. 3, pp. 174–183, 2002.
[16] S. Kaiser, "OFDM code-division multiplexing in fading channels," *IEEE Transactions on Communications*, vol. 50, no. 8, pp. 1266–1273, 2002.
[17] J. Namgoong, T. F. Wong, and J. S. Lehnert, "Subspace multiuser detection for multicarrier DS-CDMA," *IEEE Transactions on Communications*, vol. 48, no. 11, pp. 1897–1908, 2000.
[18] S. L. Miller and B. J. Rainbolt, "MMSE detection of multicarrier CDMA," *IEEE Journal on Selected Areas in Communications*, vol. 18, no. 11, pp. 2356–2362, 2000.
[19] J.-Y. Baudais, J.-F. Hélard, and J. Citerne, "An improved linear MMSE detection technique for multi-carrier CDMA systems: comparison and combination with interference cancellation schemes," *European Transactions on Telecommunications*, vol. 11, no. 6, pp. 547–554, 2000.
[20] X. Wang and H. V. Poor, *Wireless Communication Systems—Advanced Techniques for Signal Reception*, Prentice-Hall, Englewood Cliffs, NJ, USA, 2003.
[21] L.-L. Yang, W. Hua, and L. Hanzo, "Multiuser detection assisted time- and frequency-domain spread multicarrier code-division multiple-access," *IEEE Transactions on Vehicular Technology*, vol. 55, no. 1, pp. 397–405, 2006.
[22] L. Hanzo, L.-L. Yang, E.-L. Kuan, and K. Yen, *Single- and Multi-Carrier DS-CDMA*, John Wiley & Sons and IEEE Press, New York, NY, USA, 2003.
[23] H. L. V. Trees, *Optimum Array Processing*, Wiley Interscience, New York, NY, USA, 2002.
[24] S. Verdu, *Multiuser Detection*, Cambridge University Press, Cambridge, UK, 1998.
[25] H. Lutkepohl, *Handbook of Matrices*, John Wiley & Sons, Chichester, UK, 1996.
[26] S. Gray, M. Kocic, and D. Brady, "Multiuser detection in mismatched multiple-access channels," *IEEE Transactions on Communications*, vol. 43, no. 12, pp. 3080–3089, 1995.
[27] S. Glisic and P. Pirinen, "Wideband CDMA network sensitivity function," *IEEE Journal on Selected Areas in Communications*, vol. 17, no. 10, pp. 1781–1793, 1999.